



Semnan University

Mechanics of Advanced Composite Structures

journal homepage: <http://MACS.journals.semnan.ac.ir>

A Comparative Study on the Microstructure and Mechanical Properties of Al-Si-Cu/1wt %NC_P Composites after T6 Heat Treatment

F. Kamali, M. Azadi*

Faculty of Materials and Metallurgical Engineering, Semnan University, Semnan, P.O. Box: 35131-19111, Iran

KEYWORDS

Nanocomposite
Heat treatment
Hardness
Wear
Microstructure
Compressive strength

ABSTRACT

In this article, microstructural characteristics and mechanical properties of Al-Si-Cu/NC_P composites were evaluated. Reinforced nanocomposites with 1 wt% nano-clay were fabricated by the method of the stir casting. Stirring times and temperatures were variable parameters to produce specimens. Consequently, the effect of a T6 heat treatment, which contained solutioning at 490 °C for 5 hrs, quenching, and aging process at 200°C for 2 hrs, on tribological behavior and compression properties of nanocomposites was inspected. The microstructural observation was conducted by optical microscopy (OM) and the field emission scanning electron microscopy (FESEM). The acquired results demonstrated that nano-clay particles were distributed in the aluminum matrix. The range of Vickers hardness values was 123 to 158 VHN for nanocomposites. The wear resistance of nanocomposites enhanced when the stirring time and temperature increased to 4 mins and 800 °C, respectively. The best compressive mechanical properties correlated to the nanocomposite fabricated at 750 °C and stirred for 2 mins. The higher stirring time and temperature resulted in the formation of AlSiFe intermetallic phase which reduced the ultimate compressive strength.

1. Introduction

Aluminum matrix composites (MMC) are materials which are usually reinforced by ceramics particles such as, SiO₂ [1-2], Al₂O₃ [3-4], B₄C [5], SiC [6, 7], graphite [8] and TiC [9]. These materials applied in various industries, including agriculture, automotive and mining sectors, as a result of their excellent tribological and mechanical properties [10]. Aluminum matrix composites manufacturing methods can be divided into (a) solid-state processing, (b) liquid-state processing, and (3) vapor-state processing [6, 10]. The stir casting method would be proper processing as a liquid-phase method due to simplicity, low cost and good distribution of reinforcements in the matrix [1-5]. Notwithstanding, many researchers focused on manufacturing new nanocomposites, there were limited examinations about aluminum matrix composites, which were reinforced by clay-particles. These studies were summarized in the following paragraph:

Manohar et al. [11] investigated the influence of nano-clay particles on the machinability of the aluminum matrix. Their results revealed that the required work during the machining action would be increased for nanocomposites compared to the unreinforced matrix. Omole et al. [12] employed various ceramic and metal matrix composites by the powder metallurgy method and consequently evaluated the mechanical properties of composites. It was discovered that the best performance of such products would be attributed to the composite, which contained 60 wt% clay. Agbeleye et al. [13] inspected the tribological behavior of Al/clay composites applied for brake disc rotors. It was manifested that the addition of clay particles to the matrix enhanced the wear resistance and the friction coefficient of composites with respect to the AA6063 matrix. Considering the whole process, clay particles could act as reinforcement for aluminum alloys due to their high hardness and low density and friction coefficient. Therefore, since there are a few papers about adding nano-clay particles to the

* Corresponding author. Tel.: +98-910-2260629; Fax: +98-23-3154112
E-mail address: m.azadi@semnan.ac.ir

aluminum matrix, a comparative study on the investigation of Al-Si-Cu/NC_P composites fabricated by the stir casting was done in this paper. The microstructural evaluation and mechanical properties such as the hardness, the compressive strength, and wear characteristics of such nanocomposites were examined after applying a T6 heat treatment. The stirring time and the temperature of stir casting were variable parameters that changed Al-Si-Cu/NC_P composites properties as well.

2. Materials and Experiments

The chemical composition (wt %) of the aluminum matrix was measured as 7.2% Si, 3.5% Cu, 0.4 Fe, 0.4% Mn, 0.3% Mg and 88.2% Al. This result acquired by the spark optical emission spectroscopy (OES) method. Besides, nano-clay powder contained 62.3% O, 16.3% Si, 10.0% Al, 3.8% Fe, 3.0% Mg, 2.3% Na, 0.8% Ca and 0.6% Ti. It was noticeable that the applied alloy indicated proper features as a result of its excellent casting characteristics and mechanical properties [14]. Nano-clay particles with the surface area of 220-270 m²/g were applied. Before the stir casting process, nano-clay reinforcements with copper particles were mixed through a ball-milling process. A planetary ball-mill was applied for this pre-treatment. Moreover, the mixing of two powders (micro-copper particles with nano-clay particles) was operated at 30 °C for 1 hr. The argon gas purged into the ball-mill to reduce the agglomeration of the particles. In this situation, the particles wetting improvement could be achieved. Such a pre-treatment technique was reported by other studies [1-4]. More details of the milling process were found in previous studies [1-2].

The aluminum alloy was melted in an electrical resistance furnace at temperatures of 750 and 850 °C. The 1wt% of reinforcement particles were added into the aluminum. The stirring duration was 2 and 4 mins. Details of fabrication parameters for various specimens are listed in Table 1. After the casting process, the following T6 heat treatment as a new procedure for the applied alloy was manifested: (a) solutionizing at 490 °C for 5 hrs, (b) quenching in the water, and (c) aging at 200 °C for 2 hrs.

Table 1. Details of the fabrication parameters (stirring times and temperatures) for various specimens

Specimens name	Stirring temperature (°C)	Stirring time (min)
sample 750-2-H	750	2
sample 750-4-H	750	4
sample 800-2-H	800	2
sample 800-4-H	800	4

Various specimens were ground to 2000-grit and polished by alumina particles with a size of 0.5 μm. Keller's etchant was used to reveal microstructures of specimens. The optical microscopy (OM: Olympus model) and the field emission scanning electron microscopy (FESEM: FESEM- MIRA3-TSCAN) were utilized for microstructural evaluations. An X-ray diffraction method was applied to detect various phases in specimens. The radiation of CuKα was used for this examination. The scanning rate was 0.03 s⁻¹ when 2θ (Bragg angle) scan range was from 10 to 90°. The model of such spectrometer was Bruker D8.

The hardness test was operated through applying a Vickers hardness tester. The applied force was 30 N. The average value of 5 measurements was reported for each specimen. In order to inspect the tribological property of specimens, a pin-on-disc tester was applied, according to ASTM: G99-95A. Wear tests were performed by applying the normal load of 10 N. The rotation speed was 200 rpm. The wear distance was 500 m. The used pin was carbon steel with a hardness value of 271 VHN. The compression test was done according to ASTM D695. Specimens were prepared in the cylindrical form with size 10 mm in diameter and 10 mm in length, keeping the L/D ratio=1. Moreover, the porosity percent for various specimens was determined by comparing the measured density with that of their theoretical densities. Furthermore, the measured density was calculated as a result of the Archimedes principle.

3. Results and Discussion

3.1. Microstructural evaluations

The FESEM image of nano-clay particles before the ball-milling process is illustrated in Fig. 1(a). Also, the image of powders after the ball-milling process is represented in Fig. 1(b). As indicated in Fig. 1(a), the morphology of nano-clay particles was flaky-shape. Fig. 1(b) also depicts that the mean size of nano-clay particles after the ball-milling process was about 40 nm. Nano-clay particles were distributed on the copper particles surfaces. A similar distribution was discovered in other studies [3, 4].

OM images of various specimens are portraying in Fig. 2. Various phases appeared for sample 750-2-H (as given in Fig. 2(a)) and contained: (a) α- Al matrix, (b) Si particles (grey-colored areas), and (c) another phase observed in black-colored areas. The morphology of Si particles was semi-spherical. Such particles in the mentioned specimen had a uniform size.

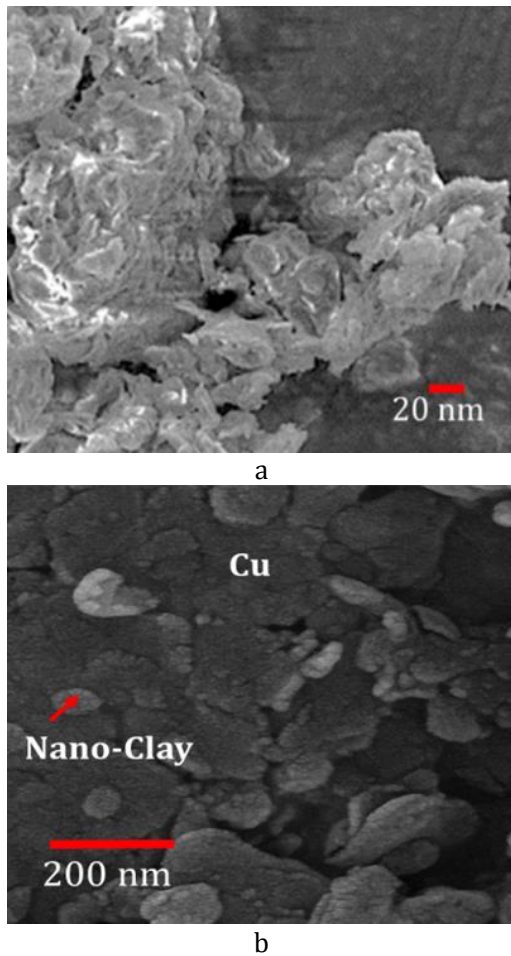


Fig. 1. FESEM images of nano-clay particles (a) before and (b) after the ball-milling process

Although the applied Al-Si matrix was a hypoeutectic alloy [15], separated Si particles were precipitated in the matrix as a result of the presence of copper in the alloy. A similar morphology was reported by other research [16]. At the stirring temperature of 750 °C, when the stirring time enhanced from 2 to 4 mins, the presence of black-phase was more obvious. Moreover, the mean size of Si particles reduced. Furthermore, there was a size distribution for such particles. The Si phase did not distribute homogeneously in the matrix, as shown in Fig. 2(b). Fig. 2(c) depicted that when the stirring temperature increased to 800 °C, the black-phase increased with the dendritic morphology. In some areas, Si particles were surrounded by such phase. Similar morphology was observed by Zhang et al. [16] as well. As given in Fig. 2(d), when the stirring time increased from 2 to 4 mins at 800 °C, a new phase (brown-colored areas) appeared in the matrix. Additionally, the size of Si particles increased obviously. Modifications in the formation of phases would be attributed to the higher temperature of the casting process plus the corporation of nano-particles in the solidification process. It was discovered that such particles would be acted as nucleation sites for the specific

phase [2]. Further, the presence of various phases with dissimilar shapes could change nanocomposite characteristics [7].

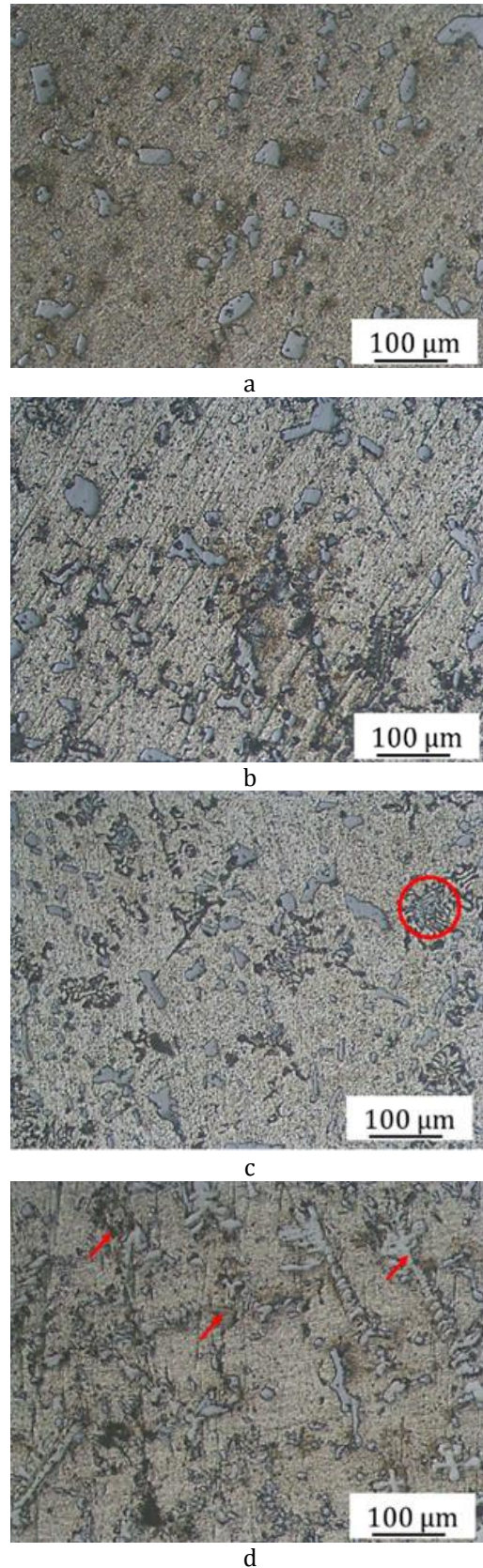


Fig. 2. OM images of nanocomposites showing various phases in the matrix; including, (a) sample 750-2-H, (b) sample 750-4-H, (c) sample 800-2-H, and (d) sample 800-4-H

FESEM images of two nanocomposites are observed in Fig. 3. Moreover, EDS results for areas A and B are indicated in Table 2. The distribution of nano-particle in the aluminum matrix decreased when the stirring temperature was 800 °C. The high stirring temperature caused to form the nano-particles cluster or colony in some areas. The size of such clustering area was lower than 100 nm. Area B reveals the presence of nano-clay particles in the matrix (area A); Despite that, for more details, the TEM images would be investigated in further study. It was discovered that the higher stirring temperature for the aluminum melt resulted in the creation of more porosities and agglomeration of ceramic particles in the metal matrix [17]. Such behavior would affect the mechanical properties of nanocomposites. Furthermore, similar events reported in another study [2]. Starra et al. [18] revealed that the state of dispersion of nano-particles in the matrix would be influenced by several factors, including inter-particle interactions and the casting temperature.

XRD patterns for two nanocomposites are shown indicated in Fig. 4. Such a pattern for the sample 750-4-H showed revealed that the black-colored areas in Fig. 2(b), were the AlSiO phase. By increasing the stirring temperature at a stirring time of 4 mins, the new phase of AlSiFe was precipitated in the matrix, which observed in the brown-colored areas in Fig. 2 (d). Furthermore, increasing the stirring temperature changed the crystallographic growth direction in aluminum grains, which affected the material properties. The most stable plane for sample 750-4-H was the plane of (111); however, such the plane changed to (220) for the sample 800-4-H. Changes in crystallographic planes for growth preferred direction was also reported by the other research [2]. Moreover, the content of the AlSiFe phase was more than AlSiO phase in the sample 800-4-H pursuant to related peaks intensities.

Micro-hardness values, wear rates, mean friction coefficient and the porosity percent are indicated in Table 3. For better discussion, results for Al-Si-Cu alloy (as a blank specimen) were compared to other specimens. All nanocomposites manifested a higher hardness (13-45%) compared to the aluminum matrix. Such an increase was as a result of the presence of reinforcement and the slower movements of dislocations in the matrix. It was reported that the addition 6 % fly ash increased the hardness of composites about 12% compared to aluminum alloy [20]. Among nanocomposites, the highest and the lowest value of hardness were related to the sample 750-2-H and the sample 800-2-H, respectively. Such event indicated that the higher stirring temperature decreased the hardness of nanocomposites.

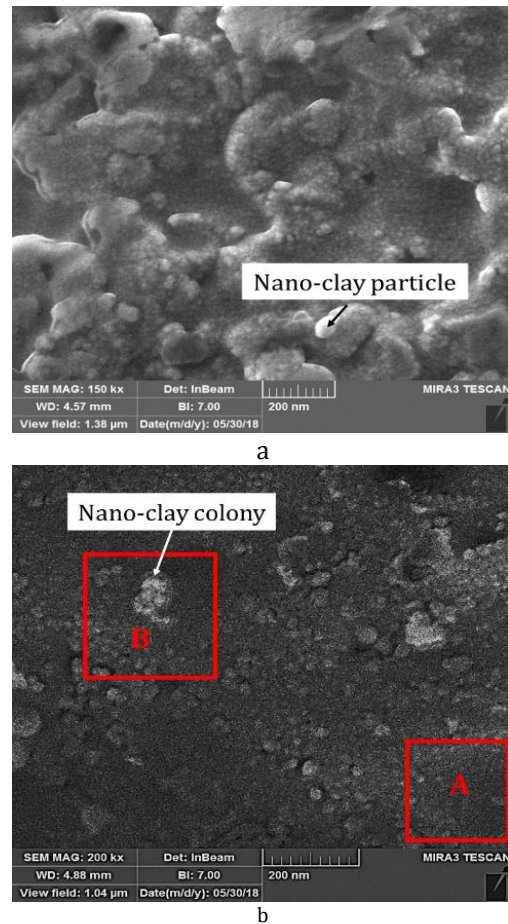


Fig. 3. FESEM images (a) nanocomposite 750-2-H and (b) nanocomposite 800-2-H

Table 2. EDS results for area A and for area B in Fig. 3(b)

	Element	W%	A%
Area A	Mg	1.70	1.65
	Al	86.47	87.66
	Si	10.95	9.93
	Fe	0.42	0.39
	Cu	0.46	0.37
Area B	O	20.62	23.73
	Mg	5.20	4.93
	Al	43.74	42.45
	Si	27.98	26.90
	Cu	2.46	1.99

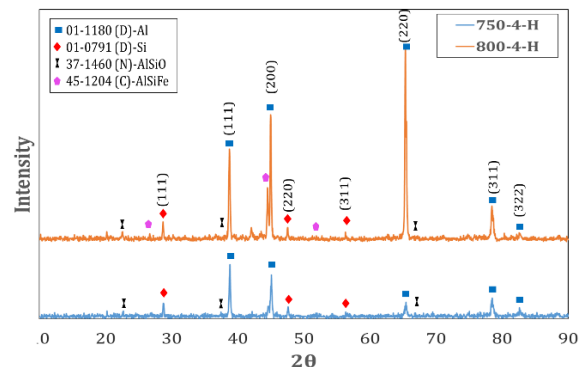


Fig. 4. XRD patterns for two nanocomposites (nanocomposite 750-4-H and 800-4-H); showing various phases

Table 3. Micro-hardness, wear rates, mean friction coefficient and porosity percent for various specimens

Specimens name	Micro-Hardness (VHN)	Wear rate (g/m.N) $\times 10^{-6}$	% porosity	Mean friction coefficient
750-2-H	158 \pm 2	7.2	1.3	0.20
750-4-H	129 \pm 2	4.8	3.5	0.40
800-2-H	123 \pm 2	5.0	4.2	0.30
800-4-H	130 \pm 2	1.3	5.1	0.15
Blank	109 \pm 2	8.2	1.1	0.65

Since the higher temperature resulted in, the higher porosities and nano-clay colonies, it caused to decrease in the hardness of nanocomposites. Additionally, changes in the microstructure affected the hardness of specimens. The presence of another intermetallic phase (AlSiFe) increased the hardness value of sample 800-4-H with respect to the sample 800-2-H. The higher stirring time and temperature raised the porosity percent as a result of the more gas entrapment in the molten aluminum [4]. Moreover, it was found that when the 8 %wt fly ash particles were added to aluminum alloy at 800 °C, the porosity content reached 5.5% [19].

It was perceptible that the applied force and the wear distance were two parameters that affected the wear resistance of material [21]. Thus, for better comparison, wear rates (instead of the weight loss) for all specimens were measured. All nanocomposites exhibited the lower wear rate with respect to the aluminum alloy as a result of the corporation of reinforcement particles in the matrix. Such particles could transfer the load during sliding action [22]. Moreover, a similar trend was reported by Dey et al. [22]. Due to Table 2, the highest and lowest wear rate for nanocomposites would be attributed to the sample 750-2-H and the sample 800-4-H, respectively. For both stirring temperatures of 750 and 800 °C, when the stirring times increased from 2 to 4 min, the wear rate decreased. This event would be related to changes in the crystallographic orientations and presence of intermetallic phases. It was discovered that the best tribological behavior for Al/SiO₂ nanocomposites was achieved when they made at a pouring temperature of 800-850 °C and were stirred for 4 min [2].

Plots of friction coefficient (COF) variations versus the wear distance for various specimens are indicated in Fig. 5. Furthermore, the mean values of COF are reported in Table 3. All nanocomposites showed the lower COF compared to the blank specimen due to the presence of nano-clay reinforcement. The highest and lowest values of COF for nanocomposites were related to the sample 750-4-H and the sample 800-4-H,

respectively. The presences of the AlSiFe phase was effective in decreasing the value of COF for the sample 800-4-H. It was discovered that when the stirring time was 4 min, the deviation of COF during wear examination was lower than the other specimens. For all samples, the occurrence of the running-in regime which was followed by the steady-state wear regime observed, similar to other results [23]. It was reported that COF was a factor which displayed the energy loss in the sliding action [21]. Therefore, the lower value of COF demonstrated lower energy loss for the sample 800-4-H. It was perceptible that the lowest COF value for Al/SiO₂ nanocomposites was reported to 0.29 [2]. Moreover, COF values for Al/fly ash composites were reported between 0.3-0.6 [24].

Plots of compressive stress versus strain for various specimens are portrayed in Fig. 6. Furthermore, extracted results (yield and ultimate strength values) from such plots are reported in Fig. 7.

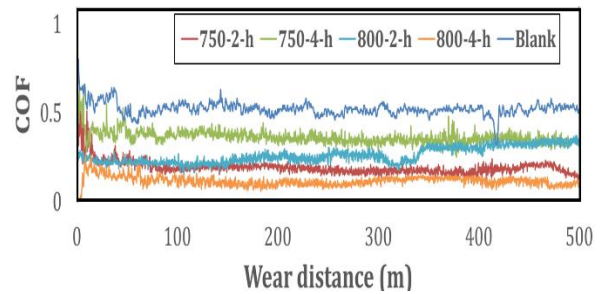


Fig. 5. Comparison of plots (COF variations versus the wear distance) for various specimens

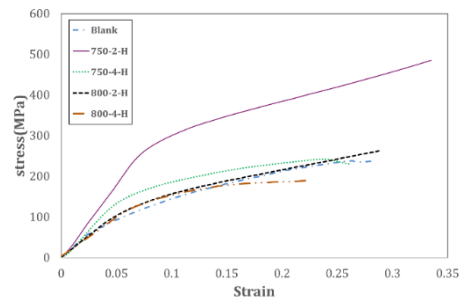


Fig. 6. Comparison of plots (stress versus strain) for various specimens in compression tests

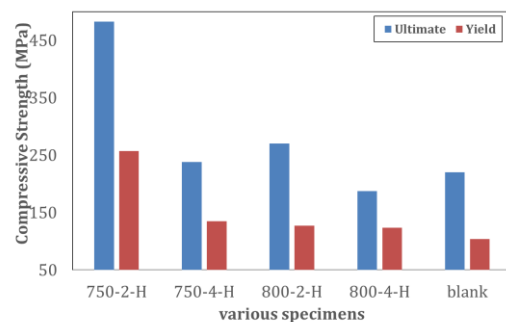


Fig. 7. Compressive strength (yield strength and ultimate strength) values for various specimens

The highest values of yield and ultimate strength, the elongation, and the toughness were related to the sample 750-4-H. Moreover, the boost in the stirring time and temperature decreased all compressive properties as a result of increasing porosity percent. Thus, the lowest value of the ultimate strength was correlated to the sample 800-4-H. In addition, there were several parameters such as the increase in the size of Si particles, the presence of AlSiFe phase, and the flaky shape of AlSiO phase lowered the yield and the ultimate strengths. Moreover, it was reported that the acicular or the flaky-morphology of Si particles were as crack initiators and decreased the mechanical properties [14]. It was discovered that the increase in the ultimate strength depended strongly on manufacturing process parameters. Various stirring times and temperatures changed the content of porosity, the formation of particle clustering, and the segregation of nano-particles at grain boundaries. Whenever the porosity content was low, and the distribution of particles was homogenous, the strength would be enhanced [7]. It was reported that agglomerated nano-particles were suitable sites for local damages and were favorable nucleation sites for cracks initiation [17]. Also, the residual stress in materials depended on the temperature from which they were cooled [25]. Thus, the higher temperature increased the local residual stress at the interface of nano-particles and the matrix which resulted in a decrease of the elongation for such nanocomposites. It was discovered that a similar alloy after the aging heat treatment without nano-particles exhibited the elongation of less than 20% and the ultimate strength of 200 MPa [26]. The boost in the ultimate compressive strength for nanocomposites was about 25-90% compared with the blank specimen. It was perceptible that all nanocomposite showed a higher yield compressive strength with respect to the aluminum alloy. It was reported that when fly ash particles were added to aluminum alloy, the ultimate compressive strength reached 400 MPa [27]. Besides, 4 wt % fly ash particles increased the ultimate compressive strength of A356 alloy [19].

For a better discussion, the parameter of square hardness to the elastic modulus ratio (H^2/E) was measured and are reported for all specimens in Table 4.

Table 4. Results of extracted parameters from compression and hardness tests for various specimens

Specimens name	Elastic modulus (GPa)	$H^2/E \times (10^{-3})$
750-2-H	2.7	9.7
750-4-H	2.1	12.3
800-2-H	1.9	11.7
800-4-H	1.8	14.1
Blank	2.0	-

The H^2/E factor could predict the wear resistance of materials. Wear rate results were consistence with H^2/E factor. Consequently, as a result of Table 4, the sample 800-4-H exhibited the highest value of the H^2/E and the best wear resistance. A similar parameter was also reported by the previous study [28]. Also, there were other parameters such as the ratio of H/E [2] and the ratio of $H/COF.E$ [29], which were suitable for the prediction of wear behavior for various materials.

4. Conclusions

In this paper, Al-Si-Cu/NC_P composites were fabricated by the stir casting method. There were two parameters that changed the properties of manufactured nanocomposites: the stirring time and temperature. A T6 heat treatment process was operated on all specimens. Consequently, tribological and compressive behaviors of specimens were examined. The outstanding results were summarized as follows:

- Various stirring temperature and times changed the morphology of Si particles in the α -Al matrix. Also, a stirring temperature of 800 °C resulted in the formation of the AlSiFe phase.
- FESEM images revealed that the distribution of nano-particle in the matrix decreased when the stirring temperature was 800 °C. The high stirring temperature caused to form of the nano-particles colony in some areas.
- The porosity percent of nanocomposites increased comparing with the aluminum alloy. Moreover, the content of porosity increased when the stirring time and temperature were 4 mins and 800 °C, respectively.
- The best compressive strength (yield and ultimate) correlated to the nanocomposite, which was stirred at 750 °C for 2 mins. This event was a result of the lower content of porosities and the semi-spherical shape of Si particles in the matrix.
- The nanocomposite, which was stirred at 800 °C for 4 mins manifested the best wear resistance since the parameter of H^2/E was the highest value for such specimen. Also, the mean value of COF for the mentioned nanocomposite was about 0.15 and was lower than other specimens. It was perceptible that all nanocomposites exhibited better tribological behaviors than the aluminum alloy.

References

- [1] Azadi M, Zolfaghari M, Rezanezhad S, Azadi M, Effects of SiO₂ Nano-particles on Tribological and Mechanical Properties of Aluminum Matrix Composites by Different Dispersion Methods, *Appl. Phys. A* 2018; 124 (5): 377-387.
- [2] Mollaei M, Azadi M, Tavakoli H, A Parametric Study on Mechanical Properties of Aluminum-Silicon/SiO₂ Nano-composites by

- a Solid-Liquid Phase Processing, *Appl. Phys. A* 2018; 124 (7): 504-514.
- [3] Akbari A K, Baharvandi H R, Mirzaee O, Nano-sized Aluminum Oxide Reinforced Commercial Casting A356 Alloy Matrix: Evaluation of Hardness, Wear Resistance and Compressive Strength Focusing on Particle Distribution in Aluminum Matrix, *Compos. Part B* 2013; 52: 262-268.
- [4] Akbari A K, Mirzaee O, Baharvandi H R, Fabrication and Study on Mechanical Properties and Fracture Behavior of Nanometric Al₂O₃ Particle-reinforced A356 Composites Focusing on the Parameters of Vortex Method, *Mater. Des.* 2013; 46; 199-205.
- [5] Mafi M, Ghasemi B, Mirzaee O, Evaluation of Hardness and Wear resistance of Nano-sized titanium-carbide-reinforced Commercially Cast Aluminum Alloy Matrices, *Mech. Adv. Compos. Struct.* 2018; 5(1):75-81.
- [6] Dyzia M, Aluminum Matrix Composite (AlSi7Mg2Sr0.03/SiCp) Pistons Obtained by Mechanical Mixing Method, *Mater.* 2018; 11(1): 42-48.
- [7] Mose J J, Dinaharan I, Sekhar S J, Prediction of Influence of Process Parameters on Tensile Strength of AA6061/TiC Aluminum Matrix Composites Produced Using Stir Casting, *Trans. Nonferrous Met. Soc. China* 2016; 26 (6): 1498-1511.
- [8] Mohanavel V, Rajan K, Kumar S S, Vijayand G, Vijayanande M S, Study on Mechanical Properties of Graphite Particulates Reinforced Aluminium Matrix Composite Fabricated by Stir Casting Technique, *Mater. Today: Proceedings* 2018; 5: 2945-2950.
- [9] Pandey U, Purohit R, Agarwal P, Dhakad S K, Rana R S, Effect of TiC Particles on the Mechanical Properties of Aluminium Alloy Metal Matrix Composites (MMCs), *Mater. Today: Proceedings* 2017; 4: 5452-5460.
- [10] Mavhungua S T, Akinlabi E T, Onitiri M A, Varachia F M, Aluminum Matrix Composites for Industrial Use: Advances and Trends, *Procedia Manu.* 2017; 7: 178-182.
- [11] Manohar H S, Chikkanna N, Gowd B U M, Effect of Addition of Nanoclay on Machinability of Al/Nanoclay Metal Matrix Composites, *Int. J. Eng. Res. App.* 2012; 2 (5): 1360-1370.
- [12] Omole O S, Barnabas A A, Akinfolarin J F, Production and Evaluation of Ceramic and Metal Matrix Composite by Powder Metallurgy, *Res. Eng. Struct. Mat.* 2015; 1(2): 73-79.
- [13] Agbeleye A A, Esezobor D E, Balogun S A, Agunsoye J O, Solis J, Neville A, Tribological Properties of Aluminium-Clay Composites for Brake Disc Rotor Applications, *J King Saud University* 2017; in press.
- [14] Elkhair M T A, Microstructure Characterization and Tensile Properties of squeeze-cast AlSiMg alloys, *Mater. Lett.* 2005; 59: 894-900.
- [15] Voort V F G, Lozano J A, The Al-Si Phase Diagram, *Microsc. Microanal.* 2009; 15(2):60-61.
- [16] Zhang D, Peng J, Huang G, Zeng D, Microstructure Evolution of Cast Al-Si-Cu Alloys in Solution Treatment, *J Wuhan University Technol. Mater. Sci. Ed.* 2008; 23(2) 184-189.
- [17] Tahamtan S, Halvae A, Emamy M, Zabihi M S, Fabrication of Al/A206-Al₂O₃ nano/micro composite by combining ball milling and stir casting technology, *Mater. Des.* 2013; 49: 347-359.
- [18] Starra F W, Douglas J F, Glotzer S C, Origin of Particle Clustering in a Simulated Polymer Nanocomposite and its Impact on Rheology, *J Chem. Phys.* 2003; 119 (3): 1777-1788.
- [19] Kulkarni SG, Meghnani J V, Lal A, Effect Of Fly Ash Hybrid Reinforcement On Mechanical Property And Density Of Aluminium 356 Alloy, *Procedia Mater. Sci.* 2014; 5: 746 -754.
- [20] Alaa M R, Dayang L M, Ishak M, Uday M, Effect of Fly Ash Addition on the Physical and Mechanical Properties of AA6063 Alloy Reinforcement, *Met* 2017; 7 (477): 711-726.
- [21] Neuville S, Matthews A, A perspective on the optimisation of hard carbon and related coatings for engineering applications, *Thin Solid Films* 2007; 515: 6619-6653
- [22] Dey A, Pandey K M, Characterization of Fly Ash and Its Reinforcement Effect on Metal Matrix Composites: A Review, *Rev. Adv. Mater. Sci.* 2016; 44: 168-181.
- [23] Vencl A, Mazeran P E, Bellafkih S, Noeld, O, Assessment of Wear Behaviour of Copper-Based Nanocomposite at the Nanoscale, *Wear* 2018; 414-415: 212-218.
- [24] Venkatachalam G, Kumaravel, A, Mechanical Behaviour of Aluminium Alloy Reinforced With SiC/FlyAsh/Basalt Composite for Brake Rotor, *Polymers Polymer Compos.* 2017; 25(3): 203-208
- [25] Ezatpour H R, Sajjadi S A, Sabzevar M H, Huang Y, Investigation of Microstructure and Mechanical Properties of Al6061-nanocomposite Fabricated by Stir Casting, *Mater. Des.* 2018; 55: 921-928.
- [26] Stanislav K, Hennadiy Z, Babett T, Aluminium Alloys for Cylinder Heads, *Mater. Geov. 2008; 55 (3): 307-317.*
- [27] Nanjayanamath N, Sugandhi R, Balanayak S, Mechanical Properties of Fly Ash Reinforced Aluminium 6061 Composite, *J. Mech. Mater. Eng.* 2011; 6: 41-45.

[28] Azadi M, Rouhaghdam A S, Nanomechanical Properties of TiN/TiC Multilayer Coatings, *Strength Mater.* 2014; 46 (1): 121-131.

[29] Neuville S, Quantum Electronic Mechanisms of Atomic Rearrangements During growth of Hard Carbon Films, *Surf. Coat. Technol.* 2011; 206: 703-726.